

# DiscoSnp-RAD: de novo detection of small variants for RAD-Seq population genomics

Jérémy Gauthier<sup>1</sup>, Charlotte Mouden<sup>1,2</sup>, Tomasz Suchan<sup>3</sup>, Nadir Alvarez<sup>4,5</sup>, Nils Arrigo<sup>4</sup>, Chloé Riou<sup>1</sup>, Claire Lemaitre<sup>1</sup>, Pierre Peterlongo<sup>Corresp. 1</sup>

<sup>1</sup> Univ Rennes, Inria, CNRS, IRISA, F-35000 Rennes, France

<sup>2</sup> INRA, BIOGECO, UMR1202, Cestas, France

<sup>3</sup> W. Szafer Institute of Botany, Polish Academy of Sciences, Krakow, Poland

<sup>4</sup> Department of Ecology and Evolution, University of Lausanne, Lausanne, Switzerland

<sup>5</sup> Natural History Museum of Geneva, Geneva, Switzerland

Corresponding Author: Pierre Peterlongo

Email address: pierre.peterlongo@inria.fr

Restriction site Associated DNA Sequencing (RAD-Seq) is a technique characterized by the sequencing of specific loci along the genome, that is widely employed in the field of evolutionary biology since it allows to exploit variants (mainly Single Nucleotide Polymorphism - SNPs) information from entire populations at a reduced cost. Common RAD dedicated tools, such as *STACKS* or *IPYRAD*, are based on all-versus-all read alignments, which require consequent time and computing resources. We present an original method, DiscoSnp-RAD, that avoids this pitfall since variants are detected by exploiting specific parts of the assembly graph built from the reads, hence preventing all-versus-all read alignments. We tested the implementation on simulated datasets of increasing size, up to 1000 samples, and on real RAD-Seq data from 259 specimens of *Chiastocheta* flies, morphologically assigned to 7 species. All individuals were successfully assigned to their species using both STRUCTURE and Maximum Likelihood phylogenetic reconstruction. Moreover, identified variants succeeded to reveal a within-species genetic structure linked to the geographic distribution. Furthermore, our results show that DiscoSnp-RAD is significantly faster than state-of-the-art tools. The overall results show that DiscoSnp-RAD is suitable to identify variants from RAD-Seq data, it does not require time-consuming parameterization steps and it stands out from other tools due to its completely different principle, making it substantially faster, in particular on large datasets.

**License:** GNU Affero general public license

[p]**Availability:** DiscoSnp-RAD belongs to the DiscoSnp repository [https://github.com/GATB/DiscoSnp/\[p\]](https://github.com/GATB/DiscoSnp/[p])

# DiscoSnp-RAD: de novo detection of small variants for RAD-Seq population genomics

Jérémy Gauthier<sup>1</sup>, Charlotte Mouden<sup>1,2</sup>, Tomasz Suchan<sup>3</sup>, Nadir Alvarez<sup>4,5</sup>, Nils Arrigo<sup>4</sup>, Chloé Riou<sup>1</sup>, Claire Lemaitre<sup>1</sup>, and Pierre Peterlongo<sup>1</sup>

<sup>1</sup>Univ Rennes, Inria, CNRS, IRISA, F-35000 Rennes, France

<sup>2</sup>INRA, BIOGECO, UMR1202, Cestas, France

<sup>3</sup>W. Szafer Institute of Botany, Polish Academy of Sciences, Kraków, Poland

<sup>4</sup>Department of Ecology and Evolution, University of Lausanne, Lausanne, Switzerland

<sup>5</sup>Natural History Museum of Geneva, Geneva, Switzerland

Corresponding author:

Pierre Peterlongo

Email address: pierre.peterlongo@inria.fr

## ABSTRACT

Restriction site Associated DNA Sequencing (RAD-Seq) is a technique characterized by the sequencing of specific loci along the genome, that is widely employed in the field of evolutionary biology since it allows to exploit variants (mainly Single Nucleotide Polymorphism - SNPs) information from entire populations at a reduced cost. Common RAD dedicated tools, such as *STACKS* or *IPYRAD*, are based on all-versus-all read alignments, which require consequent time and computing resources. We present an original method, *DiscoSnp-RAD*, that avoids this pitfall since variants are detected by exploiting specific parts of the assembly graph built from the reads, hence preventing all-versus-all read alignments. We tested the implementation on simulated datasets of increasing size, up to 1000 samples, and on real RAD-Seq data from 259 specimens of *Chiastocheta* flies, morphologically assigned to 7 species. All individuals were successfully assigned to their species using both STRUCTURE and Maximum Likelihood phylogenetic reconstruction. Moreover, identified variants succeeded to reveal a within-species genetic structure linked to the geographic distribution. Furthermore, our results show that *DiscoSnp-RAD* is significantly faster than state-of-the-art tools. The overall results show that *DiscoSnp-RAD* is suitable to identify variants from RAD-Seq data, it does not require time-consuming parameterization steps and it stands out from other tools due to its completely different principle, making it substantially faster, in particular on large datasets.

**License:** GNU Affero general public license

**Availability:** *DiscoSnp-RAD* belongs to the *DiscoSnp++* repository <https://github.com/GATB/DiscoSnp/>

## 1 INTRODUCTION

Next-generation sequencing and the ability to obtain genomic sequences for hundreds to thousands of individuals of the same species has opened new horizons in population genomics research. This has been made possible by the development of cost-efficient approaches to obtain sufficient homologous genomic regions, by reproducible genome complexity reduction and multiplexing several samples within a single sequencing run [1]. Among such methods, the most widely used over the last decade is “Restriction-site Associated DNA sequencing” (RAD-Seq). It uses restriction enzymes to digest DNA at specific genomic sites whose adjacent regions are then sequenced. This approach encompasses various methods with different intermediate steps to optimize the genome sampling, e.g. ddRAD [19], GBS [5], 2b-RAD [29], 3RAD/RADcap [11]. These methods share some basic steps: DNA digestion by one or more restriction enzymes, ligation of sequencing adapters and sample-specific barcodes, followed by optional fragmentation and fragment size selection, multiplexing samples bearing specific molecular tags, i.e. indices and barcodes, and finally sequencing. The sequencing output is thus composed of millions of

47 reads originating from all the targeted homologous loci. The usual bioinformatic steps consist in sample  
48 demultiplexing, clustering sequences in loci and identifying informative homologous variations. If a  
49 reference genome exists, the most widely used strategy is to align the reads to this reference genome  
50 and to perform a classical variant calling, focusing on small variants, Single Nucleotide Polymorphisms  
51 (SNPs) and small Insertion-Deletions (INDELs). However, RAD-Seq approaches are used on non-model  
52 organisms for which a reference genome does not exist or is poorly assembled. The fact that all reads  
53 sequenced from the same locus start and finish exactly at the same position makes it easy to compare  
54 directly reads sequenced from a same locus. To *de novo* build homologous genomic loci and extract  
55 informative variations, several methods have been developed, such as *STACKS* [2] and *PyRAD* [3], as well  
56 as its derived rewritten version *IPyRAD* [4], being the most commonly used in the population genomics  
57 community.

58 The main idea behind these approaches is to group reads by sequence similarity into clusters rep-  
59 resenting each a distinct genomic locus. Since reads originating from the same locus start and end at  
60 the same positions, they can be globally aligned, sequence variations can then be easily identified and a  
61 consensus sequence is built for each locus. The key challenge is therefore the clustering part. To do so,  
62 the classical approach relies on all-versus-all alignments. To reduce the number of alignments to compute,  
63 the clustering is first performed within each sample independently, then sample consensus are compared  
64 between samples. Nevertheless the number of alignments to perform remains very large in datasets  
65 composed of many large read sets. Importantly, analysis of RAD-Seq data is highly dependent on the  
66 chosen clustering method, the sequencing quality and the dataset composition, such as the presence of inter  
67 and/or intra-specific specimens or the number of individuals. Thus, existing tools allow customization of  
68 numerous parameters to fine-tune the analysis. Particularly, both methods have parameters controlling the  
69 granularity of clustering: the number of mismatches allowed between sequences of a same locus within  
70 and among samples for *STACKS* and the percentage of similarity for *PyRAD*. These can be arbitrarily  
71 fixed by the user, but have a significant impact on downstream analyses [24].

72 We present here *DiscoSnp-RAD*, an utterly different approach to predict *de novo* small variants (SNPs  
73 and indels) from large RAD-Seq datasets, without performing any read clustering, avoiding all-versus-all  
74 read comparisons and without relying on a critical similarity threshold parameter. *DiscoSnp-RAD* takes  
75 advantage of the *DiscoSnp++* approach [28, 18], that was initially designed for *de novo* prediction of  
76 small variants, from shotgun sequencing reads, without the need of a reference genome. The basic idea  
77 of the method is a careful analysis of the *de Bruijn graph* built from all the input read sets, to identify  
78 topological motifs, often called *bubbles*, generated by polymorphisms. Notably, those bubbles arise  
79 whatever the global similarity level between homologous reads, explaining why *DiscoSnp-RAD* is free of  
80 similarity-related parameters. Note that *STACKS2* also uses a *de Bruijn graph* approach, but in a different  
81 way, as it is used to build a so-called “*RAD-locus*” contig catalog on which reads are aligned for calling  
82 SNPs [23].

83 After validation tests on simulated datasets of increasing size, we present an application of the  
84 *DiscoSnp-RAD* implementation on double-digest RAD-Seq data (ddRAD) from a genus-wide sampling of  
85 parasitic flies belonging to *Chistocheta* genus. Using *DiscoSnp-RAD*, the 259 individuals analyzed could  
86 be assigned to their respective species. Moreover, within-species analyses focused on one of these species,  
87 identified variants revealing population structure congruent with sample geographic origins. Thus, the  
88 information obtained from variants identified by *DiscoSnp-RAD* can be successfully used for population  
89 genomic studies. The main notable difference between *DiscoSnp-RAD* and concurrent algorithms stands  
90 in its easiness to use, without any parameter to tune, and its execution time, as it is substantially faster  
91 than *STACKS* and *IPyRAD*.

## 92 2 MATERIAL AND METHODS

### 93 2.1 *DiscoSnp-RAD*: RAD-Seq adaptation of *DiscoSnp++*

94 Originally, *DiscoSnp++* was designed for finding variants from whole genome sequencing data. To  
95 adapt to the RAD-Seq context, the core algorithm of *DiscoSnp++* was extended and modified as shown  
96 Sections 2.1.1 and 2.1.2. Also, as presented Sections 2.1.3 and 2.1.4, specific features for post-processing  
97 were added to the whole pipeline.

98 ***DiscoSnp++* basic algorithm.** We first recall the fundamentals of the *DiscoSnp++* algorithm, which  
99 is based on the analysis of the *de Bruijn graph* (DBG) [20], which is a directed graph where the set of

100 vertices corresponds to the set of words of length  $k$  ( $k$ -mers) contained in the reads, and there is an oriented  
 101 edge between two  $k$ -mers, say  $s$  and  $t$ , if they perfectly overlap on  $k - 1$  nucleotides, that is to say if the  
 102 last  $k - 1$  suffix of  $s$  equals the first  $k - 1$  prefix of  $t$ . In this case, we say that  $s$  can be *extended* by the last  
 103 character of  $t$ , thus forming a word of size  $k + 1$ . A node that has more than one predecessor and/or more  
 104 than one successor is called a branching node. Small variants, such as SNPs and INDELS, generate in the  
 105 dBG recognizable patterns called “*bubbles*”. A bubble (Fig.1(a)) is defined by one *start* branching node that  
 106 has, two distinct successor nodes. From these two children nodes, two paths exist and merge in a *stop*  
 107 branching node, which has two predecessors. The type of the variant, whether it is a single isolated SNP,  
 108 several close SNPs (distant from one another by less than  $k$  nucleotides) or an INDEL, determines the  
 109 length of each of the two paths of the bubble.

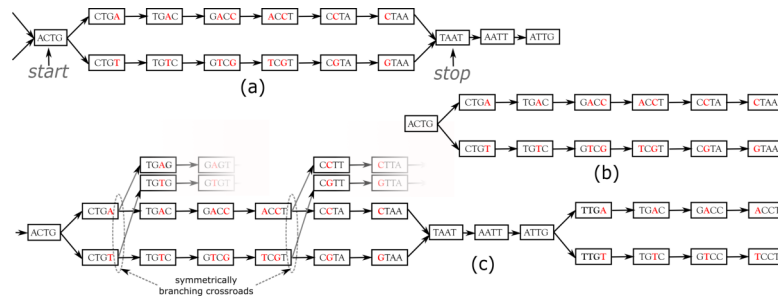


**Figure 1.** Examples of bubbles detected by SNPs in a toy de Bruijn graph, with  $k = 4$ . In (a) the bubble is complete: this corresponds to a bubble detected by *DiscoSnp++*. In (b), the bubble is symmetrically truncated: it is composed of a branching node (“ACTG”) whose two successors lead to two distinct paths that both have the same length and such that their last two nodes have no successor. Graph (c) shows an example of two bubbles from the same locus. The leftmost bubble contains two symmetrically branching crossroads.

110 *DiscoSnp++* first builds a dBG from all the input read samples combined, and then detects such  
 111 bubbles. Sequencing errors or approximate repeats also generate bubbles, that can be avoided by filtering  
 112 out kmers with a too low abundance in the read sets, and by limiting the type or number of branching  
 113 nodes along the two paths. Detected bubbles are output as pairs of sequences in fasta format. The second  
 114 main step of *DiscoSnp++* consists in mapping original reads from all samples on these sequences, in order  
 115 to compute for each variant, its read depth per allele and per read set. From this coverage information,  
 116 genotypes are inferred and variants are scored. The final output is a VCF file, where each variant is  
 117 associated to a confidence score (the *rank*) and is genotyped in each read set, thanks to its allele coverages  
 118 (see [18, 28]).

119 In *DiscoSnp-RAD*, these two main steps have been modified to adapt to the RAD-seq context and  
 120 an additional third step has been developed in order to cluster the variants per locus and to output this  
 121 information in the final VCF file. In short, *DiscoSnp-RAD 1/* constructs the de Bruijn graph and detects  
 122 bubbles whose topology correspond to SNPs or indels, *2/* maps back reads on found bubble sequences,  
 123 thus assessing the read coverage per allele and per read set, and *3/* performs clustering on predicted  
 124 sequences. Those three steps are described in the three following sections.

### 125 2.1.1 Bubble detection with *DiscoSnp-RAD*

126 **A novel RAD-specific bubble model.** In *DiscoSnp++*, variants distant from less than  $k$  bp from a  
 127 genomic extremity could not be detected, as associated bubbles do not open and/or close. This effect  
 128 is negligible in the whole genome sequencing context, however, in the RAD-Seq context, sequenced  
 129 genomic regions are limited to a hundred or to a few hundreds nucleotides (the read size), and thus a large  
 130 amount of variants are likely to be located at the extremities of the loci. For instance, with reads of length  
 131 100bp, and  $k = 31$  (which is a usual  $k$  value), on average 62% of the variants are located in the first or last  
 132  $k$  nucleotides of a locus and cannot be detected by *DiscoSnp++*.

133 In the RAD-Seq context, all reads sequenced from the same locus start and end exactly at the same  
 134 position. Thus, variants located less than  $k$  bp from loci extremities generate what we call *Symmetrically*  
 135 *Truncated Bubbles* (Fig.1(b)). Such bubbles start with a node which diverges into two distinct paths that  
 136 do not meet back, such that both of them cannot be extended because of absence of successor and both

137 paths have exactly the same length. Symmetrically, a variant located less than  $k$  bp apart from loci start  
 138 generates a bubble that is right closed, but that starts with two unconnected paths of the same length.

139 To further increase specificity of the truncated bubble model, we also constrain the last 3-mer of  
 140 both paths to be identical. Although this prevents the detection of variants as close as 3 bp from a  
 141 locus extremity, this enables to identify correctly the type of detected variant. Indeed, when the last  
 142  $L$  nucleotides of two locus sequences are different, several mutation events could have taken place in  
 143 the genome resulting in the same observed differences: either an indel (of any size) or  $L$  successive  
 144 substitutions or a combination of the two types. When  $L$  is small, all events may be equally parsimonious  
 145 and we prefer to report none of these instead of a wrong one. Note that this does not prevent to detect loci  
 146 containing such variants. The value  $L$  was set to 3 because it leads to a relatively low loss of recall (6%  
 147 with reads of length 100), while the probability of observing by chance three successive matches is low  
 148 ( $= \frac{1}{4^3} \approx 1.56\%$ ). Note that this issue is also present in any mapping or clustering based approaches.

149 The core of the *DiscoSnp-RAD* algorithm SNP bubble detection is sketched in Algorithm 1. Al-  
 150 gorithm 1 is intentionally simplified and hides the process enabling to detect SNPs separated by less  
 151 than  $k$  nucleotides and INDELS. The full and detailed algorithm is proposed in supplementary materials.  
 152 Basically, after the graph construction, we loop over all its branching nodes (line 2), each branching  
 153 node is then considered as a potential bubble extremity. The pair of paths that can be generated from  
 154 this branching node are explored (lines 5 to the end). Notably, the two paths are created simultaneously  
 155 nucleotide by nucleotide. The extension stops 1/ if the extension is impossible (line 10, if there exists no  
 156 nucleotide  $\alpha$  such that  $kmer_1$  and  $kmer_2$  can be extended with  $\alpha$ ); or 2/ if the bubble closes (line 11); or  
 157 3/ if the bubble is truncated (line 7).

158 **Dealing with entangled bubbles.** As RAD-Seq data often include a large number of individuals, this  
 159 is likely that many SNPs are close to each other (separated by less than  $k$  nucleotides), and that a large  
 160 number of distinct haplotypes co-exist. This situation generates bubbles that are imbricated in one another  
 161 and what we call “*Symmetrically Branching Crossroads*” (SBCs), as shown in Fig.1(c). SBCs appear  
 162 when more than one unique character may be used during extension. All possible extensions are explored  
 163 (line 12) in presence of SBCs. However, we limit the maximal number of traversals of SBCs per bubble  
 164 to 5 by default (line 14). This value has been chosen as larger values lead to longer computation time,  
 165 larger false positive calls (due to repetitive genomic regions), while not changing significantly recall, as  
 166 shown in the results. Depending on the user choice, we also propose a “high\_precision” mode in which  
 167 bubbles containing one or more SBC(s) are not detected.

---

**Algorithm 1** Simplified overview of the *DiscoSnp-RAD* SNP bubble detection (Indel bubble detection omitted)

---

```

1: Create a de Bruijn graph from all (any number  $\geq 1$ ) read set(s)
2: for Each right branching  $k$ -mer in the graph start do
3:   for each couple of successor  $kmer_1, kmer_2$  of  $k$ -mer start do
4:      $nb\_sym\_branching=0$ 
5:     while True do
6:       Extend  $kmer_1$  and  $kmer_2$  with  $\alpha \in \{A, C, G, T\}$ 
7:       if Both  $kmer_1$  and  $kmer_2$  have no successors then
8:         if last 3 characters from  $kmer_1$  and  $kmer_2$  are equal then
9:           Output bubble and break
10:        if Extension is impossible then break
11:        if  $kmer_1 = kmer_2$  then Output bubble and break
12:        if two or more possible extending nucleotides  $\alpha$  then
13:          Increase  $nb\_sym\_branching$ 
14:          if  $nb\_sym\_branching > 5$  then break
15:        else Explore recursively all possible extensions

```

---

### 168 2.1.2 Computing allele coverage and inferring genotypes

169 In this second step, original reads from all samples are mapped on all bubble sequences, in order to provide  
 170 the read coverage per allele and per read set. Importantly, this mapping step allows non-exact mapping,  
 171 allowing a high number of substitutions (up to 10 by default), except on the polymorphic positions of

172 the bubble. As shown in results, this choice enables to maximize the sensibility by allowing numerous  
173 variations, while maintaining a high precision as no substitution is authorized on variant positions.

174 These coverage information enables to infer individual genotypes and to assign a score (called *rank*) to  
175 each variant enabling to filter out potential false positive variants. Genotypes are inferred only if the total  
176 coverage over both alleles is above a *min\_depth* threshold (by default 3), using a maximum likelihood  
177 strategy with a classical binomial model [18, 16], otherwise the genotype is indicated as missing (“./”).  
178 Variants with too many missing genotypes (by default more than 95 % of the samples) are filtered out.

179 Paralogous genomic regions represent a major issue in population genomic analyses as DNA sections  
180 arising from duplication events can be aggregated in the same locus and thus, might encompass alleles  
181 coming from non orthologous loci. Allele coverage information across many samples can be used to  
182 filter out many of such paralog-induced variants. As the latter tend to occur in all the samples, their allele  
183 frequency is thus non discriminant between samples. An efficient scoring scheme, called the *rank* value in  
184 *DiscoSnp++*, reflects such discriminant power of variants. First, we define the Phi coefficient of a given  
185 variant for a given pair of samples, as  $\sqrt{\frac{\chi^2}{n}}$ , with  $\chi^2$  being the chi-squared statistics computed on the allele  
186 read counts contingency table for this pair of samples, and  $n$  being the sum of read counts in this table.  
187 This is an association measure between two binary variables (here allele vs sample) ranging between  
188 0 (no association) and 1 (maximal association). Then, when more than two samples are compared, the  
189 rank value is obtained by computing the Phi coefficient of all possible pairs of samples and retaining the  
190 maximum value. We have shown in previous work [28, 18] that paralog-induced variants are likely to  
191 generate bubbles in the dBG but with very low rank values ( $< 0.4$ ) contrary to real variants. This filter is  
192 particularly effective when many samples are compared, as in the RAD-seq context. Thus, by default,  
193 *DiscoSnp-RAD* discards all variants with such low rank values.

### 194 **2.1.3 Clustering variants per locus**

195 During the bubble detection phase, several independent bubbles can be predicted for the same RAD  
196 locus. For instance, Fig.1(c) shows a toy example of a the dBG graph associated to a locus. In this  
197 case, *DiscoSnp-RAD* detects two bubbles, that give no sign of physical proximity. In several population  
198 genomics analyses, such proximity information can be useful, such as in population structure analyses,  
199 where this is recommended to select only one variant per locus. In order to recover this information of  
200 locus membership, we developed a post-processing method to cluster predicted variants per locus.

201 The method uses the fact that *DiscoSnp-RAD* is parameterized to output bubbles together with their  
202 left and right contexts in the graph, which correspond to the paths starting from each extreme node and  
203 ending at the first ambiguity (ie. a node with not exactly one successor). For instance, the leftmost  
204 bubble of Fig.1.c is output as sequences ACTG**ACCT**AATg and ACTG**TCGTA**ATg, where we represent  
205 the context sequences in lower case, and rightmost bubble of the same figure is output as sequences  
206 taATTG**ACCT** and taATTG**TCCT**.

207 By definition of these extensions, if a given locus contains several variants, each bubble of this locus  
208 extended with its left and right contexts shares at least one  $k - 1$ -mer with at least one other so extended  
209 bubble of the same locus. For instance, the pairs of sequences of the two bubbles shown Fig.1.c share the  
210  $k - 1$ -mer TAA (among others).

211 We exploit this property to group all bubbles per locus. For doing so, we create a graph in which a  
212 node is a bubble (represented by its pair of sequences including the extensions), and there is an undirected  
213 edge between two nodes  $N_i$  and  $N_j$  if any of the two sequences of  $N_i$  shares at least one  $k - 1$ -mer with  
214 any of the two sequences of  $N_j$ . Those edges are computed using *SRC\_linker* [15].

215 Finally, we partition this graph by connected component. Each connected component contains all  
216 bubbles for a given locus and this information is reported in the vcf file. By default, clusters containing  
217 more than 150 variants are discarded, as they are likely to aggregate paralogous variants from repetitive  
218 regions.

### 219 **2.1.4 Various optional filtering options**

220 The output of *DiscoSnp-RAD* is a VCF file containing predicted variants along with various information,  
221 such as their genotypes and allele read counts in all samples, their *rank* value and the cluster ID (locus)  
222 they belong to. This enables to apply custom filters at the locus level, as well as any variant level  
223 classical RAD-Seq filters (such as the minimal read depth to call a genotype or the minimal minor  
224 allele frequency to keep a variant). Several such RAD-seq filtering scripts are provided along with

225 the main program ([https://github.com/GATB/DiscoSnp/tree/master/discoSnpRAD/](https://github.com/GATB/DiscoSnp/tree/master/discoSnpRAD/post-processing_scripts)  
226 [post-processing\\_scripts](https://github.com/GATB/DiscoSnp/tree/master/discoSnpRAD/post-processing_scripts)).

## 227 2.2 Testing environment

228 The tests were performed on the GenOuest ([genouest.org](http://genouest.org)) cluster, on a node composed of 40 Intel  
229 Xeon core processors with speed 2.6 GHz and 252 GB of RAM.

## 230 2.3 Validation on simulated datasets

231 Note that all scripts used for simulations and validations are publicly available [https://doi.org/](https://doi.org/10.5281/zenodo.3724518)  
232 [10.5281/zenodo.3724518](https://doi.org/10.5281/zenodo.3724518).

233 **Simulation protocol.** RAD loci from *Drosophila melanogaster* genome (dm6) were simulated by  
234 selecting 150 bp on both sides of 43,848 PstI restriction sites resulting in 87,696 loci. Several populations,  
235 each composed of several diploid individuals were simulated as follows. For each simulated population,  
236 SNPs were randomly generated at a rate of 1%. A first subset of them (70%) was introduced in all samples  
237 from the population and represent shared polymorphism. The rest of these SNPs (30%) were distributed  
238 between samples by a random picking of 10% of them and assigned to each sample. For each sample,  
239 10% of the assigned SNPs, shared and sample specific, are introduced in only one of the homologous  
240 chromosomes to simulate heterozygosity. This process was repeated to generate from 5 to 50 populations  
241 each composed of 20 individuals. Finally, between 2,109,900 SNPs for 100 samples, and 2,547,337 SNPs  
242 for 1,000 samples, were generated. Forward 150bp reads were simulated on right and left loci, with 1%  
243 sequencing errors, with 20X coverage per individual (the complete pipeline is given in Supplementary  
244 Figure 1).

245 **Evaluation protocol.** For estimating the result quality, predicted variants were localized on the *D.*  
246 *melanogaster* genome and output in a vcf file. To do so, we used the standard protocol of *DiscoSnp++*  
247 when a reference genome is provided, using BWA-mem [14]. The predicted vcf was compared to the  
248 vcf storing simulated variant positions to compute the amount of common variants (true positive or TP),  
249 predicted but not simulated variants (false positive or FP) and simulated but not predicted variants (false  
250 negative or FN). Recall is then defined as  $\frac{\#TP}{\#TP+\#FN}$ , and precision as  $\frac{\#TP}{\#TP+\#FP}$ .

251 **Comparison with other tools.** For comparisons, *STACKS* v2.4 and *IPyRAD* v0.7.30 were run on the  
252 simulated datasets. *STACKS* stacks were generated *de novo* (`denovo_map.pl`), with a minimum of 3  
253 reads to consider a stack (-m 3). On the simulated dataset composed of 100 samples, five values of the  
254 parameter -M governing stack merging (ie. 4, 6, 8, 10, and 12) were tested. On the remaining datasets, the  
255 parameter -M was fixed to 6 following r80 method [17]. All other parameters were set to default values.  
256 Similarly, *IPyRAD* was run using five values of clustering threshold on the dataset composed of 100  
257 samples (ie. 0.75, 0.80, 0.85, 0.90 and 0.95) and then fixed to 0.80, following r80 method [17], for larger  
258 datasets. The other parameters have been kept at the default values. Then, *de novo* tags from *STACKS* and  
259 loci from *IPyRAD* were mapped to the *D. melanogaster* genome using BWA-mem and variant positions  
260 were transposed on the genome positions with a custom script.

## 261 2.4 Application to real data from *Chiastocheta* species

262 **Data origin.** Tests on real data were performed on ddRAD reads previously obtained for the phylogenetic  
263 study of seed parasitic pollinators from the genus *Chiastocheta* (Diptera: Anthomyiidae). The dataset  
264 corresponds to the sequencing of 259 individuals sampled from 51 European localities generated by  
265 Lausanne University, Switzerland [26] (<https://www.ebi.ac.uk/ena/data/view/PRJEB23593>). A total of  
266 608,367,380 reads were used for the study with an average of 2.3 Million reads per individual.

267 **Variant prediction and filtering.** *DiscoSnp-RAD* was run with default parameters, searching for at most  
268 five variants per bubble. For *IPyRAD* the same parameters as in the Suchan *et al.* study [26] have been  
269 applied including a percentage of identity of 75% for the clustering and a minimum coverage of 6. For  
270 *STACKS* we applied a minimum coverage by stack (-m) of 3, a maximum number of mismatches allowed  
271 among sample (-M) of 8 and a maximum number of mismatches allowed between sample (-n) of 8. On  
272 the output vcf from each tools, downstream classical filters were applied to follow as much as possible  
273 the filters used in the Suchan *et al.* study [26]: a minimum genotype coverage of 6, a minimal minor  
274 allele frequency of 0.01 and a minimum of 60% of the samples with a non missing genotype for each

275 variant. These filters remove less informative variants or those with an allele specific to a very small  
 276 subset of samples. These filters were also applied at the intra-specific level in one of the seven sampled  
 277 *Chiastocheta* species, i.e. *C. lophota*, on the same *DiscoSnp++* output.

278 **Population genomic analyses.** The species genetic structure was inferred using STRUCTURE [21]  
 279 v2.3.4. This approach requires unlinked markers, thus only one variant by locus, randomly selected, has  
 280 been kept. The STRUCTURE analysis was carried on the datasets generated by each tool. Simulations  
 281 were performed with genetic cluster number ( $K$ ) set from 1 to 10. Best  $K$  was identified using Evanno's  
 282 method [7]. We used 20,000 MCMC iterations after a burn-in period of 10,000. The output is the posterior  
 283 probability of each sample to belong to each of the possible clusters. For *C. lophota* species, a multivariate  
 284 analysis were used to investigate intra-specific genetic structure using adegenet R package [12].

285 **Phylogenomic analyses.** Maximum likelihood (ML) phylogenetic reconstruction was performed  
 286 on a whole concatenated SNP dataset using GTRGAMMA model with the acquisition bias correc-  
 287 tion [13]. We applied rapid Bootstrap analysis with the extended majority-rule consensus tree stopping  
 288 criterion and search for best-scoring ML tree in one run, followed by ML search, as implemented in  
 289 RAxML v8.2.11 [25].

## 290 3 RESULTS

### 291 3.1 Results on simulated data

292 *DiscoSnp-RAD* was first run on several simulated RAD-Seq datasets composed of an increasing number of  
 293 samples (from 100 to 1,000) in order to validate the approach, to evaluate its speed and efficiency and to  
 294 compare it with the other clustering approaches. This experiment shows that *DiscoSnp-RAD* predictions  
 295 are accurate with a good compromise between recall and precision (see Figure 2).

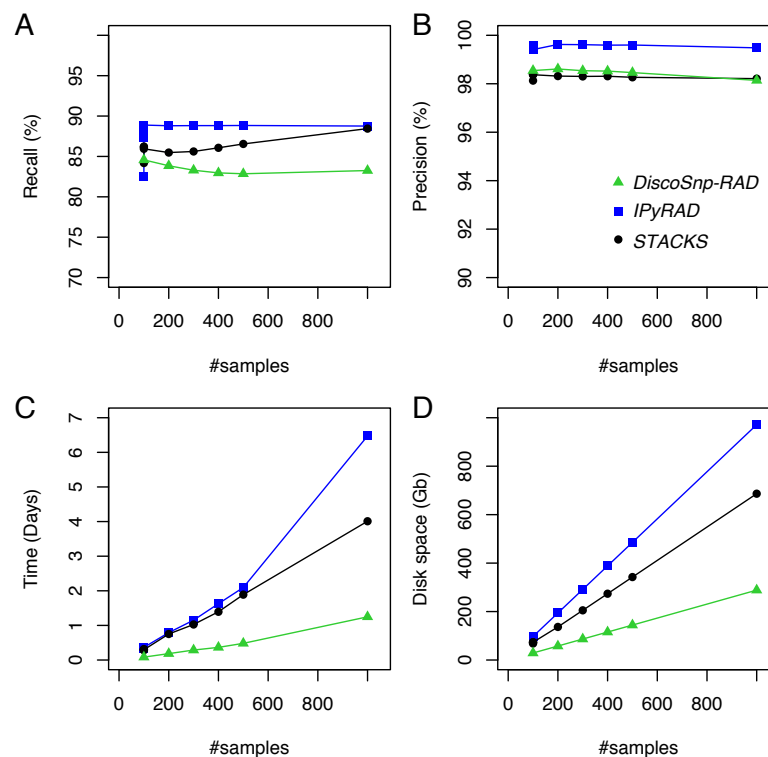


**Figure 2.** Recall (A), precision (B), time (C) and space (D) evolution on simulated data with different sampling sizes. For the sampling of 100 samples, five parameter sets were tested for *IPyRAD* and *STACKS* (see Material and Methods for details).

296 On average, 84.6 % of the simulated variants are recovered with very few false positive calls, i.e.

297 reaching a precision of 98.5 % on average. Importantly, these performances are not impacted by the  
298 number of input samples in the dataset. For instance, recall varies from 84.6% to 83.3% between the  
299 smallest and the largest datasets (100 vs 1.000 samples), and precision from 98.1 % to 98.5%.

300 By comparison with other tools, for each of the tested population sizes, recall and precision are  
301 comparable between tools, with typically a recall lower than *STACKS* and *IPyRAD* and an intermediate  
302 precision, lower than *IPyRAD* and higher than *STACKS*. The loss of recall may be explained by the fact  
303 that *DiscoSnp-RAD* voluntarily does not detect the variants within 3 bp of each locus end (see Methods).  
304 The amount of predicted loci are similar between all tools (Supplementary Table 2). The main differences  
305 between the tools concern the run time and the disk space usage. These differences increase with the  
306 number of samples in the dataset. For instance, on the largest dataset composed of 1,000 samples  
307 *DiscoSnp-RAD* is more than 3 times faster than *STACKS* and more than 5 times faster than *IPyRAD*.  
308 Moreover, if we consider the cumulative time required to test different parameters for *STACKS* and  
309 *IPyRAD*, i.e. five sets of parameters for each tool, *DiscoSnp-RAD*, without parameter setting is more than  
310 15 times faster than *STACKS* and more than 25 times faster than *IPyRAD*. Regarding the disk space used  
311 by the tool during the process, *DiscoSnp-RAD* requires only a small amount of space compared to the  
312 other tools. Full RAM memory, disk usage, and computation times of *DiscoSnp-RAD* are provided in  
313 Supplementary Table 1.

314 **Robustness with respect to parameters.** A major advantage of *DiscoSnp-RAD* stands in the fact  
315 that it does not require fine parameter tuning. This is an important point as other state-of-the-art tools  
316 are extremely sensible to their parameters, especially those directly linked to the expected sequence  
317 divergence, and require time consuming processes to set them properly [24]. In *DiscoSnp-RAD*, the main  
318 parameter is the size of  $k$ -mers, used for building the dBG. As shown Figure 3, *DiscoSnp-RAD* results  
319 are robust with respect to  $k$ , the main parameter, and its fine choice is thus not crucial. This figure also  
320 highlights the results robustness with respect to other parameters such as the maximal number of predicted  
321 SNPs per bubble (5 by default), the maximal number of substitutions authorized when mapping reads on  
322 bubble sequences (10 by default), and the maximal number of symmetrically branching crossroads (also 5  
323 by default). Concerning this last parameter, Figure 3 also shows the advantages of the “high\_precision”  
324 mode which sets this parameter to zero, leading to a precision of nearly 100%.

### 325 3.2 Results on real data

326 In this section, we present an application of the *DiscoSnp-RAD* implementation on ddRAD sequences  
327 obtained from the anthomyiid flies from the *Chiastocheta* genus. In this genus, classical mitochondrial  
328 markers are not suitable for discriminating the morphologically described species [6]. Although RAD-  
329 sequencing dataset phylogenies supported the species assignment [26], the interspecific relationships  
330 between the taxa could not be resolved with high confidence due to high levels of incongruences in gene  
331 trees [9, 26]. The dataset is composed of 259 sequenced individuals from 7 species. Results obtained on  
332 *DiscoSnp-RAD* were compared to the prior work of Suchan and colleagues, based on *pyRAD* analysis [26].  
333 In addition, we provide a performance benchmark of *STACKS*, *IPyRAD* and *DiscoSnp-RAD* run on this  
334 dataset.

335 **Recovering all *Chiastocheta* species.** Variant calling was run on the 259 *Chiastocheta* samples with  
336 *DiscoSnp-RAD*. Before filtering, 115,920 SNPs were identified. After filtering, 4,364 SNPs, located in  
337 1,970 clusters, were retained and used for population genomic analyses. The total number of clusters is  
338 coherent with the 1,672 loci from Suchan *et al.* [26].

339 Then, following the requirements of the STRUCTURE algorithm, only one variant per cluster was  
340 retained, resulting in a dataset composed of 1,970 SNPs. The most likely value of  $K$  is 7 (data not shown)  
341 and corresponds to the seven species described in [26]. STRUCTURE successfully assigned samples  
342 to the seven species, consistent with the morphological species assignment and previously published  
343 results [26] (Fig.4). The assignment values represent the probability with which STRUCTURE assigns a  
344 sample to a cluster, depending on the information carried by the variants. The assignment values are high  
345 with an average of 0.992 (sd 0.022) across samples and a minimum assignment of 0.810. These values are  
346 comparable to the assignment values obtained by Suchan *et al.* [26] with an average of 0.977 (sd 0.042)  
347 and a minimum of 0.685. Genetic structure has also been investigated for the two other tools and give  
348 very similar population assignments (Supplementary Figure 2).

349 The phylogeny realized with RAxML on the 4,364 SNPs obtained after filtering, is congruent with the

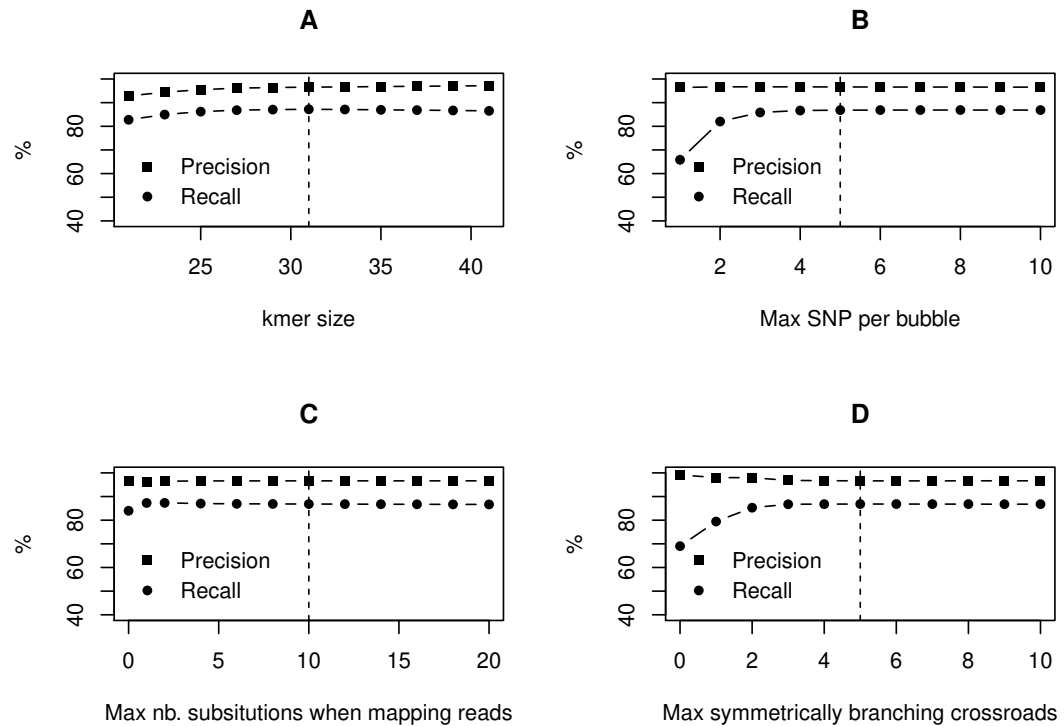


**Figure 3.** Recall and precision on simulated data of 100 samples using *DiscoSnp-RAD* with respect to **A.**  $k$ -mer sizes, **B.** maximal number of authorized SNP per bubble, **C.** maximal number of authorized substitutions while mapping reads on predicted variants sequences, and **D.** maximal number of symmetrically branching crossroads. Dashed vertical line represents on each plot the chosen default value.

350 one obtained by Suchan and colleagues [26] (Fig.4). The internal branches separating the seven species  
 351 are well supported by high bootstrap values.

352 **Recovering phylogeographic patterns.** To assess the utility of *DiscoSnp-RAD* results for investigating  
 353 the intra-specific genetic structure, we then focused the analysis on 40 samples of *C. lophota* species.  
 354 From the same vcf file obtained with the 259 samples, the 40 *C. lophota* samples were extracted and the  
 355 same filters, i.e. MAF, missing etc., were applied on this *C. lophota* dataset.

356 We obtained 1,306 SNPs by selecting one variant per locus extracted from 4,364 variants identified in  
 357 this species. The multivariate analysis of this dataset identify three populations comprising respectively  
 358 31, 5 and 4 samples. (Fig.4). Notably, the genetic structure follows the geographic distribution of the  
 359 samples, with samples from one population originating from western locations, another population from  
 360 eastern locations and an intermediate population. Geographic structuring is the most frequent structuration  
 361 factor observed in population genetics, pointing to the geographical isolation of divergent lineages. This  
 362 clear geographic structuring is another hint that *DiscoSnp-RAD* recovers real biogeographic signal.

363 **Breakthrough in running time.** *DiscoSnp-RAD* run on the 259 *Chiastocheta* samples took about 30  
 364 hours. This comprises the whole process from building the dBG to obtaining the final filtered vcf file  
 365 with 1 SNP per locus. To compare the *DiscoSnp-RAD* performances with *STACKS* and *IPyRAD* on real  
 366 data, we ran each of these tools using default parameters on the 259 *Chiastocheta* samples and measured  
 367 running time and maximum memory usage. The difference is remarkable, *DiscoSnp-RAD* is more than  
 368 4.65 times faster than *STACKS* (running time 138 hours) and 2.8 times faster than *IPyRAD* (running time  
 369 82 hours) to perform the whole process. Moreover, contrary to *DiscoSnp-RAD*, *STACKS* and *IPyRAD*  
 370 should be run several times to explore the parameters which represent a considerable amount of time and  
 371 memory. For instance, in Suchan *et al.* [26], *IPyRAD* was run with 5 different combinations of parameter

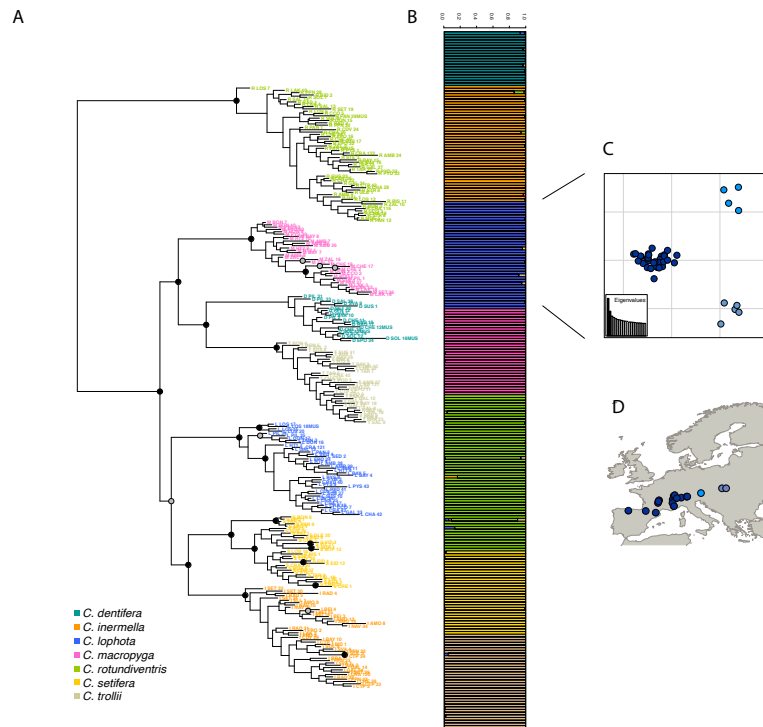


**Figure 4.** A. RAxML phylogeny realized on all variants predicted by *DiscoSnp-RAD*. Bootstrap node supports > 80 are shown denoted by gray dots, bootstrap node supports > 90 are shown denoted by black dots. B. STRUCTURE results obtained with SNP only and all variants on the seven *Chiastocheta* species. C. Plot of the two first PC from a multivariate analysis on *C. lophota* samples and, D. their geographic distribution.

372 values, *DiscoSnp-RAD* being thus 14 times faster than *IPyRAD*.

#### 373 4 DISCUSSION

374 ***DiscoSnp-RAD* efficiency.** *DiscoSnp-RAD* produced relevant results on ddRAD data from *Chiastocheta*  
 375 species. SNPs identified allowed us to successfully i) distinguish the seven species based on the STRUC-  
 376 TURE algorithm, and ii) reconstruct the phylogenetic tree of the genus, congruent with the previously  
 377 published one [26]. Moreover, on the intra-specific scale, we obtained geographically meaningful results  
 378 within *C. lophota* species. The variants identified by *DiscoSnp-RAD* can be used to study the species or  
 379 population genetic structure and could be used to investigate deeper the mechanisms at the origin of this  
 380 structure such as potential gene flow between populations or their demographic histories. In addition,  
 381 *DiscoSnp-RAD* is also able to identify INDELS [18]. They were not used in this study but are available  
 382 for users.

383 Furthermore, the use of *DiscoSnp-RAD* presented considerable advantages in the run-time, and  
 384 parameters choice, compared to other common *de novo* RAD analysis tools, as described below.

385 **Run-time.** The use of *DiscoSnp-RAD* dramatically decreased the overall time for discovering and  
 386 selecting relevant variants, as compared to other tools. This is made possible thanks to the use of a unique  
 387 indexing data structure, the dBG built from all the reads. To build this graph, reads do not need to be  
 388 compared to each other. *DiscoSnp-RAD* speed depends on the graph size and at a lesser extend on the  
 389 number of reads. Importantly, it is not expected to increase quadratically with the dataset size. This can  
 390 likely be anticipated that with the drop of sequencing costs, RAD projects will grow in size, either by  
 391 using higher frequency cutting enzymes to obtain a dense genome screening, by increasing the sequencing  
 392 depth to compensate sequencing variation or by increasing the number of samples. In this context,  
 393 *DiscoSnp-RAD* will more easily scale to such very large datasets.

394 **Easy parameter choice.** Another substantial advantage of using *DiscoSnp-RAD* is the fact that param-  
395 eters are not directly linked to the level of expected divergence of the compared samples. In fact, they  
396 impact the number and type of detected variants, but are not related to the subsequent clustering step. As  
397 a result, same parameters can be used whatever the type of analysis (for example, intra or inter-specific),  
398 contrasting with classical tools in which parameters govern loci recovering. Indeed, in *STACKS*, the  
399 parameters governing the merge of the stacks can compromise the detection of relevant variants if they are  
400 not adapted to the studied dataset [24]. Therefore, the authors recommend to perform an exploration of  
401 the parameter space before downstream analyses [17]. This is extremely time consuming, up to one month  
402 as confessed by the authors [22], and may not always result in interpretable conclusions. In *IPyRAD*, the  
403 similarity parameter for clustering also impacts variant detection, and usually several values have to be  
404 tested to choose the best, as exemplified by Suchan and colleagues who tested five different values [26].

405 **By-locus assembly.** *DiscoSnp-RAD* output is a vcf file including pseudo-loci information, that allows  
406 the application of standard variant filtering pipelines. One next objective is to recover loci consensus  
407 sequences, that could be used for phylogenetic analysis based on full locus sequences. This could be  
408 achieved by performing local assemblies per individual, from all bubbles contained in a cluster.

409 **Potential applications.** *DiscoSnp-RAD* can handle all types of RAD data including original RAD-Seq,  
410 GBS, ddRAD, etc. In addition it is able to use reads 2 from original RAD-Seq data that are often difficult  
411 to analyse. These reads do not start and finish at the same position. Properly recovery of loci is therefore  
412 not possible with read stacking approaches. This problem does not exist when using *DiscoSnp-RAD*, and  
413 variants present in reads 2 can also be called. Indeed, the *DiscoSnp-RAD* method, being not based on  
414 stacks of reads, is able to detect any variants that generate bubble motifs in the dBG, thus even if present  
415 in reads whose starting positions differ.

416 This ability of *DiscoSnp-RAD* to handle reads that do not necessary start at the same genomic position  
417 makes it particularly well suited to analyze the datasets produced by another group of genome-reduction  
418 techniques, namely sequence capture approaches [10]. In these techniques, DNA shotgun libraries are  
419 subject to enrichment using short commercially-synthesized [8] or in-house made [27] DNA or RNA  
420 fragments acting as 'molecular baits', that hybridize and allow separation of homologous fragments  
421 from genomic libraries. One of such promising approaches is HyRAD, a RAD approach combining  
422 the molecular probes generated using ddRAD technique and targeted capture sequencing, designed for  
423 studying old and/or poor quality DNA, likely to be too fragmented for RAD-sequencing [27]. In HyRAD,  
424 capturing randomly fragmented DNA results in reads not strictly aligned and covering larger genomic  
425 regions than RAD-Seq. Therefore RAD tools can not be used to reconstruct such loci, and the current  
426 analysis consists in building loci consensuses from reads, and then calling variants by mapping back the  
427 reads on it. The use of *DiscoSnp-RAD* should simplify this process in a single *de novo* calling step, well  
428 adapted to the specificities of data generated by reduction approaches: many compared samples, high  
429 polymorphism and clustering by locus.

## 430 5 CONCLUSION

431 We propose *DiscoSnp-RAD*, an original method dedicated to the *de-novo* analyse of RAD-Seq data. We  
432 have shown that on simulated data, the quality of the results is comparable to those obtained by state-of-the  
433 art tools, *STACKS* and *IPyRAD*. On real data, *DiscoSnp-RAD* provides relevant results, enabling the  
434 structuring at inter- and intra-level species, accurate enough for recovering the phylogeographic patterns.

435 Due to its methodological approach which is utterly different from existing methods, *DiscoSnp-RAD*  
436 drastically reduces computation times and memory requirements. Another key difference stands in the  
437 fact that *DiscoSnp-RAD* does not rely on fine tuning of parameters, contrary to existing methods that rely  
438 on critical parameters, as those related to the input sequence similarity.

## 439 ACKNOWLEDGMENTS

440 Authors thank Camille Marchet for her precious help on the clustering implementation. Computations  
441 have been made possible thanks to the resources of the Genouest infrastructures. This work was supported  
442 by the French ANR-14-CE02-0011 SPECREP grant.

## REFERENCES

- 443
- 444 [1] Andrews, K., Good, J., R Miller, M., Luikart, G., and A Hohenlohe, P. (2016). Harnessing the power  
445 of radseq for ecological and evolutionary genomics. *Nature Reviews Genetics*, 17:81–92.
- 446 [2] Catchen, J., Hohenlohe, P. A., Bassham, S., Amores, A., and Cresko, W. A. (2013). Stacks: an analysis  
447 tool set for population genomics. *Molecular Ecology*, 22(11):3124–3140.
- 448 [3] Eaton, D. A. R. (2014). Pyrad: assembly of de novo radseq loci for phylogenetic analyses. *Bioinforma-*  
449 *tics*, 30(13):1844–1849.
- 450 [4] Eaton, D. A. R. and Overcast, I. (2020). ipyrad: Interactive assembly and analysis of RADseq datasets.  
451 *Bioinformatics*. btz966.
- 452 [5] Elshire, R. J., Glaubitz, J. C., Sun, Q., Poland, J. A., Kawamoto, K., Buckler, E. S., and Mitchell, S. E.  
453 (2011). A robust, simple genotyping-by-sequencing (gbs) approach for high diversity species. *PLOS*  
454 *ONE*, 6(5):1–10.
- 455 [6] Espíndola, A., Buerki, S., and Alvarez, N. (2012). Ecological and historical drivers of diversification  
456 in the fly genus *Chiastocheta pokorny*. *Molecular Phylogenetics and Evolution*, 63(2):466–474.
- 457 [7] EVANNO, G., REGNAUT, S., and GOUDET, J. (2005). Detecting the number of clusters of individuals  
458 using the software structure: a simulation study. *Molecular Ecology*, 14(8):2611–2620.
- 459 [8] Faircloth, B. C., McCormack, J. E., Crawford, N. G., Harvey, M. G., Brumfield, R. T., and Glenn, T. C.  
460 (2012). Ultraconserved elements anchor thousands of genetic markers spanning multiple evolutionary  
461 timescales. *Systematic Biology*, 61(5):717–726.
- 462 [9] Gori, K., Suchan, T., Alvarez, N., Goldman, N., and Dessimoz, C. (2016). Clustering genes of  
463 common evolutionary history. *Molecular Biology and Evolution*, 33(6):1590–1605.
- 464 [10] Grover, C. E., Salmon, A., and Wendel, J. F. (2012). Targeted sequence capture as a powerful tool for  
465 evolutionary analysis I. *American Journal of Botany*, 99(2):312–319.
- 466 [11] Hoffberg, S. L., Kieran, T. J., Catchen, J. M., Devault, A., Faircloth, B. C., Mauricio, R., and Glenn,  
467 T. C. (2016). Radcap: sequence capture of dual-digest radseq libraries with identifiable duplicates and  
468 reduced missing data. *Molecular Ecology Resources*, 16(5):1264–1278.
- 469 [12] Jombart, T. (2008). adegenet: a R package for the multivariate analysis of genetic markers. *Bioinforma-*  
470 *tics*, 24(11):1403–1405.
- 471 [13] Leaché, A. D., Banbury, B. L., Felsenstein, J., de Oca, A. N.-M., and Stamatakis, A. (2015). Short  
472 tree, long tree, right tree, wrong tree: new acquisition bias corrections for inferring snp phylogenies.  
473 *Systematic Biology*, 64(6):1032–1047.
- 474 [14] Li, H. and Durbin, R. (2009). Fast and accurate short read alignment with Burrows-Wheeler transform.  
475 *Bioinformatics*, 25(14):1754–1760.
- 476 [15] Marchet, C., Limasset, A., Bittner, L., and Peterlongo, P. (2016). A resource-frugal probabilistic  
477 dictionary and applications in (meta)genomics. *CoRR*, abs/1605.08319.
- 478 [16] Nielsen, R., Paul, J. S., Albrechtsen, A., and Song, Y. S. (2011). Genotype and SNP calling from  
479 next-generation sequencing data. *Nature Reviews Genetics*, 12:443–451.
- 480 [17] Paris, J. R., Stevens, J. R., and Catchen, J. M. (2017). Lost in parameter space: a road map for stacks.  
481 *Methods in Ecology and Evolution*, 8(10):1360–1373.
- 482 [18] Peterlongo, P., Riou, C., Drezen, E., and Lemaitre, C. (2017). Discosnp++: de novo detection of  
483 small variants from raw unassembled read set(s). *bioRxiv*.
- 484 [19] Peterson, B. K., Weber, J. N., Kay, E. H., Fisher, H. S., and Hoekstra, H. E. (2012). Double digest  
485 radseq: An inexpensive method for de novo snp discovery and genotyping in model and non-model  
486 species. *PLOS ONE*, 7(5):1–11.
- 487 [20] Pevzner, P. A., Tang, H., and Tesler, G. (2004). De novo repeat classification and fragment assembly.  
488 *Genome Research*, 14(9):1786–1796.
- 489 [21] Pritchard, J. K., Stephens, M., and Donnelly, P. (2000). Inference of population structure using  
490 multilocus genotype data. *Genetics*, 155(2):945–959.
- 491 [22] Rochette, N. C. and Catchen, J. M. (2017). Deriving genotypes from RAD-seq short-read data using  
492 Stacks. *Nature Protocols*, 12(12):2640–2659.
- 493 [23] Rochette, N. C., Rivera-Colón, A. G., and Catchen, J. M. (2019). Stacks 2: Analytical methods for  
494 paired-end sequencing improve radseq-based population genomics. *Molecular Ecology*, 28(21):4737–  
495 4754.
- 496 [24] Shafer, A. B. A., Peart, C. R., Tusso, S., Maayan, I., Brelsford, A., Wheat, C. W., and Wolf, J. B. W.  
497 (2017). Bioinformatic processing of rad-seq data dramatically impacts downstream population genetic

- 498 inference. *Methods in Ecology and Evolution*, 8(8):907–917.
- 499 [25] Stamatakis, A. (2014). Raxml version 8: a tool for phylogenetic analysis and post-analysis of large  
500 phylogenies. *Bioinformatics*, 30(9):1312–1313.
- 501 [26] Suchan, T., Espíndola, A., Rutschmann, S., Emerson, B. C., Gori, K., Dessimoz, C., Arrigo, N.,  
502 Ronikier, M., and Alvarez, N. (2017). Assessing the potential of rad-sequencing to resolve phylogenetic  
503 relationships within species radiations: The fly genus *Chiastocheta* (Diptera: Anthomyiidae) as a case  
504 study. *Molecular Phylogenetics and Evolution*, 114:189–198.
- 505 [27] Suchan, T., Pitteloud, C., Gerasimova, N. S., Kostikova, A., Schmid, S., Arrigo, N., Pajkovic, M.,  
506 Ronikier, M., and Alvarez, N. (2016). Hybridization capture using rad probes (hyrad), a new tool for  
507 performing genomic analyses on collection specimens. *PLOS ONE*, 11(3):1–22.
- 508 [28] Uricaru, R., Rizk, G., Lacroix, V., Quillery, E., Plantard, O., Chikhi, R., Lemaitre, C., and Peterlongo,  
509 P. (2015). Reference-free detection of isolated SNPs. *Nucleic Acids Research*, 43(2):1–11.
- 510 [29] Wang, S., Meyer, E., Mckay, J., and Matz, M. (2012). 2b-rad: A simple and flexible method for  
511 genome-wide genotyping. *Nature Methods*, 9:808–10.